

Insight into Molecular Basis of Curing of $[PSI^+]$ Prion by Overexpression of 104-kDa Heat Shock Protein (Hsp104)^{*[5]}

Received for publication, September 9, 2011, and in revised form, October 30, 2011. Published, JBC Papers in Press, November 11, 2011, DOI 10.1074/jbc.M111.302869

Christopher W. Helsen and John R. Glover¹

From the Department of Biochemistry, University of Toronto, Toronto, Ontario M5S 1A8, Canada

Background: All yeast prions are dependent on Hsp104 for propagation but only the $[PSI^+]$ prion is cured by Hsp104 overexpression.

Results: Deletion of a small region of Sup35, the protein determinant of $[PSI^+]$, alters its interaction with Hsp104 and diminishes prion curing but not propagation.

Conclusion: Hsp104-mediated curing of $[PSI^+]$ is dependent on a site that is accessible in the context of the prion aggregate that can interact with Hsp104 and regulate its ATPase activity.

Significance: Understanding the molecular basis of prion remodeling by Hsp104 may have implications for understanding how protein aggregation associated with disease could be mitigated by molecular chaperones.

Yeast prions are a powerful model for understanding the dynamics of protein aggregation associated with a number of human neurodegenerative disorders. The AAA+ protein disaggregase Hsp104 can sever the amyloid fibrils produced by yeast prions. This action results in the propagation of “seeds” that are transmitted to daughter cells during budding. Overexpression of Hsp104 eliminates the $[PSI^+]$ prion but not other prions. Using biochemical methods we identified Hsp104 binding sites in the highly charged middle domain of Sup35, the protein determinant of $[PSI^+]$. Deletion of a short segment of the middle domain (amino acids 129–148) diminishes Hsp104 binding and strongly affects the ability of the middle domain to stimulate the ATPase activity of Hsp104. In yeast, $[PSI^+]$ maintained by Sup35 lacking this segment, like other prions, is propagated by Hsp104 but cannot be cured by Hsp104 overexpression. These results provide new insight into the enigmatic specificity of Hsp104-mediated curing of yeast prions and sheds light on the limitations of the ability of Hsp104 to eliminate aggregates produced by other aggregation-prone proteins.

$[PSI^+]$ is a prion-like element in yeast based on two metastable conformations of the protein Sup35 (1). In $[psi^-]$ cells, the soluble conformer of Sup35 participates along with Sup45 (2) in the termination of translation at termination codons and nonsense codons alike. In $[PSI^+]$ cells, the majority of Sup35 molecules are sequestered in self-assembling fibrillar aggregates. In these cells the fidelity of translation termination is sufficiently reduced to permit significant read-through of nonsense codons. By influencing the expression of the yeast proteome, the capacity to switch between $[PSI^+]$ and $[psi^-]$ can be advantageous for survival of cells facing different environmental challenges (3, 4) and may be evolutionarily conserved (5). However,

recent analysis of newly induced $[PSI^+]$ suggests that strains of $[PSI^+]$ can be deleterious or lethal (6).

During budding, Sup35 fibrils, also known as “seeds” or “propagons,” partition into daughter cells where they continue to recruit newly synthesized soluble Sup35 conferring a suppression phenotype identical to that of the mother cell. An important factor in the stable cytoplasmic inheritance of yeast prions is the maintenance of a sufficient population of propagons to ensure partitioning of at least some of them into the daughter cell during budding. Mathematical modeling of the rate loss of $[PSI^+]$ after prion propagation is blocked suggests that the number of $[PSI^+]$ propagons is in the range of 500–1000 per cell and that about one-third of these are inherited by the daughter cell during budding (7). Although pre-existing fibrils continue to expand by recruiting soluble Sup35, each fibril must be broken or severed once or twice during the cell cycle to sustain the pool of propagons. The formation of propagons is dependent on the thermotolerance factor Hsp104. Both deletion of Hsp104 (8) and inhibition of Hsp104 function by guanidinium (9) result in loss of the $[PSI^+]$ prion.

Hsp104 is an AAA+ protein with two nucleotide-binding domains in each protomer and which forms a ring-shaped homohexamer (10, 11). Hsp104 contributes to the survival of thermally damaged cells by helping to refold misfolded, aggregated proteins (12). Hsp104 and its bacterial ortholog ClpB contact misfolded proteins trapped in aggregates by binding to exposed polypeptide loops or termini and, in a ATP-driven cycle, extracts proteins from the aggregate by unfolding and threading the amino acid chain through a central cavity or channel formed by the assembled hexamer (13, 14). Proteins freed from the aggregate are able to refold upon release from Hsp104. It has been proposed that the same mechanism used to extract proteins from aggregates of thermally denatured proteins could be used to sever fibrillar aggregates associated with prions (15).

Depletion of Hsp104 increases the size of visible GFP-tagged Sup35 aggregates in $[PSI^+]$ cells (16) and increases the size of SDS-resistant Sup35 particles (17) consistent with its proposed role in fibril severing. The extraction of a single protomer can

* The work was supported by Canadian Institutes of Health Research Operating Grant MOP-86754 (to J. R. G.).

[5] This article contains supplemental Table S1 and Figs. S1–S3.

¹ To whom correspondence should be addressed: Rm. 5302 Medical Sciences Bldg., 1 King's College Circle, Toronto, Ontario M5S 1A8, Canada. Tel.: 416-978-3008; Fax: 416-978-8548; E-mail: john.glover@utoronto.ca.

be expected to disrupt the local stability of the amyloid-like extended β -sheet that forms the backbone of the prion fibril and result in severing in a manner analogous to the proposed mechanism of microtubule severing by the AAA+ protein spastin (18). In addition to $[PSI^+]$, the propagation of nearly all known yeast prions, including $[PIN^+]$ (19), $[URE3]$ (20), $[OCT1^+]$ (21), $[SWT^+]$ (22), and $[MOT3^+]$ (23), is dependent on Hsp104.

In contrast to the role of Hsp104 in the propagation of most prions, only the $[PSI^+]$ prion is cured by Hsp104 overexpression. Although Hsp104 is critical for propagation of prions when expressed at modest levels in unstressed cells, Hsp104 overexpression can be expected to enhance the frequency of extraction of Sup35 protomers from fibrils thereby reducing the number of propagons and the probability of transmission to daughter cells during budding. This idea is supported by *in vitro* experiments in which high concentrations of Hsp104 can disintegrate preformed Sup35 fibrils to the extent that they no longer nucleate fibril growth (24, 25). However, *in vivo* evidence suggests that whereas the amount of soluble Sup35 does increase during the early stages of Hsp104 overexpression (17) or when Hsp104 expression is induced by heat shock (26), SDS-resistant Sup35 particles actually increase in size. Thus curing by Hsp104 overexpression may involve the formation of large particles that exceed a size threshold that is postulated to be required for efficient partitioning of propagons to daughter cells (27) prior to separation and cytokinesis.

Regardless of the end product of the reaction, the molecular basis of the exceptional Hsp104/Sup35 interaction that leads to $[PSI^+]$ curing is unknown. One possibility is that the amyloid-like fibrils produced by other prion-forming proteins are resistant to Hsp104-mediated curing because the protomers in these structures are more tightly integrated into fibrils by a network of hydrogen bonds and other interactions thereby acquiring a higher physical stability than structures formed by Sup35. Nonetheless, because they are dependent on Hsp104 for propagation, they must be susceptible to fragmentation at a rate, however low, necessary to maintain a suitable population of propagons. Another possibility is that Sup35 has an intrinsically stronger interaction with Hsp104 than other prionogenic yeast proteins. To gain insight into the latter possibility we set out to determine possible sites of interaction between Hsp104 and Sup35.

It is logical that Hsp104 must have access to part of Sup35 that is exposed on the $[PSI^+]$ prion. Proton exchange experiments (28) and accessibility of residues to chemical modification reagents (29) indicate that the solvent inaccessible core of the $[PSI^+]$ prion is composed of an Asn/Gln-rich region of Sup35 (residues 1–40) and extends at least partially into a region of 5.5 imperfect nonapeptide repeats (residues 41–97). Comparison of electron micrographs of fibrils formed *in vitro* by the combined N- (amino acids 1–123) and M-domains (amino acid 124–253) of Sup35 (NM)² with those formed by

full-length Sup35 suggests that the N-domain forms the core amyloid fiber, whereas the globular C-domain (amino acids 254–685) is displayed along the fiber axis tethered to the amyloid core by the M-domain (30).

In this work we investigated the hypothesis that the Sup35 M-domain (Md) is involved in propagation and curing of $[PSI^+]$ by Hsp104. We show that Md inhibits $[PSI^+]$ propagation *in vivo* and inhibits chaperone-dependent remodeling of the Sup35 NM-domain *in vitro*. We mapped this interaction to a 20-amino acid segment of Sup35 (residues 129–148) that is required for stimulation of the ATPase activity of Hsp104 and that strongly inhibits binding to Hsp104 of a model unfolded protein. An NM-domain lacking this region is resistant to chaperone-dependent remodeling *in vitro*. *In vivo*, prions maintained by Sup35 Δ 129–148 are larger than their full-length counterparts and are lost more rapidly following inhibition of Hsp104 by guanidinium HCl, indicating that fewer propagons are maintained in these cells. Finally, Sup35 Δ 129–148 prions are not cured by Hsp104 overexpression. These observations represent the first time that a functionally important interaction site between Hsp104 and Sup35 has been localized, providing insight into the molecular basis of Hsp104-mediated curing unique to $[PSI^+]$.

EXPERIMENTAL PROCEDURES

Plasmid Construction—All oligonucleotide sequences are listed in supplemental Table S1. For the bacterial expression of the NM-domain, pET3aNM was constructed by PCR using pJC45NM (30) as a template with primers NM (A and B) and insertion of the PCR product into pET3a (Novagen) using NdeI and BamHI sites. NMY106C was constructed using primers NMY106C (B) and NM (C). The PCR product was digested with NcoI and EcoRV and used to replace the NM coding region in pJC40NM creating pJC40NMY106C. For the bacterial expression of Md, the DNA segment encoding Sup35 amino acid residues 105–253 was amplified from pET3aNM using primers M22A and M22B. The PCR product was inserted into pET22b using NdeI and EcoRI sites to create plasmid pET22bM. A bacterial expression vector for NM Δ 129–148 was created by overlap extension PCR using primers NM Δ 129–148 (A and B) in combination with primers NM (A and B) used to generate pET3aNM Δ 129–148. These primers also introduce flanking AgeI and BstBI restriction sites, resulting in Q118E and S150T substitutions. For bacterial expression of Md Δ 129–148, primers M22 (A and B) were used with pET3a NM Δ 129–148 as template and the PCR product was cloned into pET22b with NdeI and XhoI. For the bacterial expression of Md(105–163) and Md(164–253), primers 105 (A and B) or 253 (A and B), respectively, were used to amplify segments from pET22bM. The PCR products were inserted into pET22b using NdeI and XhoI to produce pET22bMd(105–163) and pET22bMd(164–253). For bacterial expression of MdCtC and Md Δ 129–148CtC primers MC (A and B) were used to amplify from pET22bMd and pET22bMd Δ 129–148, respectively. NdeI- and XhoI-digested PCR products were subcloned into pET22b to produce pET22bMdCtC and pET22bMd Δ 129–148CtC.

To create a high-copy number plasmid for the copper-inducible expression of Md in yeast we first PCR amplified the *CUP1*

² The abbreviations used are: NM, combined N- (amino acids 1–123) and M-domains (amino acid 124–253) of Sup35; ThT, thioflavin T; Md, Sup35 M-domain; fRCMLa, fluorescently labeled reduced carboxymethylated α -lactalbumin.

Hsp104-mediated Curing of $[PSI^+]$ Prion

promoter from pCAUHSEM104 using primers CUP1 (A and B). The *GAL1* promoter was excised from p425GAL1 (31) with *SacI* and *BamHI* and replaced with the digested PCR product to create p425CUP1. The Md coding sequence was amplified from pET22bM using primers MCUP (A and B). The PCR product was inserted into p425CUP1 using *BamHI* and *XhoI*. To create a *LEU2*-marked plasmid expressing Sup35 Δ 129–148 for plasmid shuffling, a *BclI* and *PstI* fragment was isolated from pET3aNM Δ 129–148 and subcloned into pRS315SUP35 (32) generating pRS315sup35 Δ 129–148. For the purpose of inserting other DNAs in place of the 129–148 encoding segments this strategy created flanking restriction sites that created amino acid substitutions Q118E and S150T. We found that these substitutions in the context of full-length Sup35 had no effect on the suppression phenotype of $[PSI^+]$ or Hsp104-mediated curing (data not shown).

For the bacterial expression of huHsp70, a cleavable His tag was amplified from a expression plasmid pET-WT-hsp70 (33) using primers huHSP70 (A and B) and inserted into pPROEXb using a *BamHI* and *SacI* restriction digest. To ensure fidelity of amplified sequences, all cloned PCR products were sequenced completely at The Centre for Applied Genomics (The Hospital for Sick Children, Toronto, Canada). The sequence of the huHsp70 matched that of human HSPA1A (NCBI reference sequence: NM_005345.5).

Protein Expression and Purification—Hsp104, Hsp104^{Trap}, Hsp104^{E285A}, and Ydj1 were expressed and purified as previously described (34–37). His-tagged HuHsp70 was purified following the same procedure as used for Hsp104. All purification procedures were performed at 4 °C.

NM, NM Δ 129–148, and NMY106C were expressed in BL21(DE3) containing the pRARE plasmid overnight at 25 °C. Cells suspended in lysis buffer (150 mM NaCl, 40 mM HEPES, pH 7.4) containing protease inhibitors (1 μ g/ml each pepstatin A, leupeptin, and aprotinin, and 0.1 mM phenylmethanesulfonyl fluoride) were incubated in a boiling water bath for 25 min. The boiled lysate was cleared by centrifugation at 20,000 \times g for 30 min and all subsequent purification steps were carried out at room temperature. For purification of NM and its derivatives, the supernatant was precipitated with 50% of saturation (\sim 2 M) ammonium sulfate. The resulting pellet was solubilized in 40 mM citrate, pH 5.0, 1.6 M ammonium sulfate, 8 M urea, filtered, and applied to a column of HiTrap Phenyl-Sepharose fast flow (GE Healthcare). The column was washed with at least 20 column volumes of the same buffer and eluted with the same buffer without ammonium sulfate. Protein was buffer exchanged into 40 mM Tris-HCl, pH 8.4, 10 mM NaCl, 8 M urea on a G-25 column (GE Healthcare) and subsequently bound to a HiTrap Q HP column (GE Healthcare), washed with at least 20 column volumes, and eluted with 40 mM Tris-HCl, pH 8.4, 250 mM NaCl, 8 M urea. The protein was aliquoted and precipitated with 9 volumes of cold methanol. Pellets were dried and stored at -80 °C. For purification of the NMY106C protein, 5 mM β -mercaptoethanol was added to all buffers.

For the purification of Md and Md Δ 129–148, Md(164–253), MdCtC, and Md Δ 129–148CtC, proteins were expressed in BL21(DE3) containing the pRARE plasmid overnight at 25 °C. Cell pellets were resuspended in 40 mM Tris-HCl, pH 8.4, 10

mM NaCl and lysed by incubation in a boiling water bath for 25 min. The lysate was cleared at 20,000 \times g for 30 min. Cleared lysate was loaded onto HiTrap Q HP (GE Healthcare), washed with at least 20 column volumes of 40 mM Tris-HCl, pH 8.4, 60 mM NaCl, and eluted with the same buffer containing 250 mM NaCl. The protein was dialyzed against sterile water, aliquoted, flash frozen, and stored at -80 °C. For the C-terminal Cys derivatives, 5 mM β -mercaptoethanol was included in all buffers.

For purification of Md(105–163), bacterial cells were boiled in 5 mM potassium phosphate buffer, pH 6.8. Cleared lysate was applied to a ceramic hydroxyapatite column Type I (Bio-Rad), which was washed with 50 mM potassium phosphate buffer and eluted with a gradient of 50–500 mM potassium phosphate buffer. Protein-containing fractions were pooled, dialyzed against sterile water, aliquoted, flash frozen, and stored at -80 °C.

Yeast Strains and Manipulation—Plasmid shuffling experiments were performed in strain 780-1D (*MATa*, *kar1-1*, *SUQ5*, *ade2-1*, *his3 Δ 202*, *leu2 Δ 1*, *trp1 Δ 63*, *ura3-52*, *sup35::KanMX* (pJ533: *URA3-SUP35*), $[PSI^+]$) and a $[psi^-]$ version of the same strain (38). Yeast strains were transformed using a standard procedure (39) with *LEU2*-marked plasmids for the expression of Sup35 and the *HIS3*-marked plasmid for the galactose-inducible expression of Hsp104. Yeast containing all three plasmids were selected on minimal medium lacking leucine, uracil, and histidine. To force the loss of the *URA3*-marked plasmid, cells were grown to saturation, diluted, and regrown to saturation in minimal medium with 1 mg/ml of 5'-fluoroorotic acid. Cells were plated for selection of the two remaining plasmids and checked for the loss of *URA3* by streaking onto plates lacking uracil. For curing by Hsp104 overexpression, expression was induced in 2% (w/v) galactose and 0.03% (w/v) glucose, cells were grown to saturation, washed in sterile water, and plated on selective plates with 2% (w/v) glucose.

To monitor curing of $[PSI^+]$ by Md expression, the yeast strain OT55 (*MATa*, *ade1-14UGA*, *his3*, *leu2*, *trp1-289UAG*, *ura3*, $[PSI^+]$) (40) was transformed with p425CUP1Md or p425CUP1 with no insert. Both strains were cultured in minimal selective medium with 50 μ M CuSO₄ and repeatedly diluted into 3 ml of fresh medium. At regular intervals cells were removed, washed in sterile water, and plated on selective medium, lacking CuSO₄. Curing was assessed by colony color with pale cells considered to be $[PSI^+]$ and red colonies $[psi^-]$.

For curing by guanidinium (Gdm), cells were grown in selective media containing 5 mM GdmHCl. Cells were kept in a perpetual growing state by repeatedly diluting cultures that had reached saturation into fresh selective media containing 5 mM GdmHCl. Periodically aliquots were plated on selective media without Gdm added. Curing was scored after 5 days using the colony color as an indicator.

Gel Electrophoresis and Western Blotting—Yeast were lysed in 25 mM HEPES-KOH, pH 7.5, 150 mM NaCl, 10 mM EDTA with 1 μ g/ml each of pepstatin A, leupeptin, aprotinin, and 0.1 mM PMSF. Cell debris was removed by centrifugation at 400 \times g for 2 min at 4 °C and the protein concentrations of the supernatants were determined using the Bio-Rad Protein Assay (Bio-Rad) and equalized prior to the addition of sample buffer (50

mM Tris-HCl, pH 6.8, 100 mM DTT, 2% (w/v) SDS, 10% (v/v) glycerol). After SDS-PAGE separation, protein was transferred to a PVDF membrane (Pall Corp.) and blocked in 20 mM Tris-HCl, pH 7.6, 137 mM NaCl, 0.05% (w/v) milk powder. Sup35 was detected using an anti-N-domain polyclonal antibody (gift from Susan Lindquist) at a dilution of 1:500. Md was detected using an anti-Md antibody (Santa Cruz Bioscience) at 1:250 dilution. Hsp104 was detected with a rabbit polyclonal antibody (37). For loading control rabbit anti-yeast alcohol dehydrogenase antibodies were used (1:5000).

For prion particle analysis, lysates were incubated in sample buffer at either 38 or 99 °C (boiled) for 25 min. These were submitted to SDS-PAGE as described above or run on 2% (w/v) agarose gels in TAE buffer (40 mM Tris-HCl, pH 8.0, 1 mM EDTA, 20 mM Na-acetate) with 0.1% (w/v) SDS using a horizontal gel apparatus. Protein concentrations were either determined using the Bio-Rad protein assay or the Micro BCA™ Protein assay kit (ThermoFisher Scientific).

For SDS resistance of NM fibrils formed *in vitro*, samples were heated in sample buffer at 38 or 99 °C (boiled) for 20 min and subjected to electrophoresis on 12.5% polyacrylamide resolving gels and stained with Coomassie Blue. SDS-resistant NM does not enter the resolving gel (41). For thermal stability experiments, NM or NMΔ129–148 fibrils were heated to the indicated temperature for 20 min before electrophoresis.

Fluorophore Labeling of Proteins—Purified NMY106C was incubated for 30 min at room temperature with 10 mM dithiothreitol (DTT). DTT was removed and the buffer was changed to 6 M GdmHCl using a G-25 column. A 20-fold molar excess of acrylodan (Invitrogen) dissolved in dimethyl sulfoxide was added and the reaction was incubated overnight at room temperature. Unbound acrylodan was removed by desalting on G-25. Labeled protein was aliquoted, flash frozen, and stored at –80 °C. Labeling efficiency was determined by measuring acrylodan absorbance at 372 nm (extinction coefficient = 844,114 M⁻¹ cm⁻¹) relative to the protein concentration determined at 280 nm (extinction coefficient = 28,310 M⁻¹ cm⁻¹). Labeling efficiency was >50%.

Purified MdCtC or MdΔ129–148CtC domain was treated with 1 mM DTT to reduce Cys residues and then buffer exchanged on G-25 columns (GE Healthcare) into 6 M GdmHCl, 40 mM Tris-HCl, pH 7.3. A 5-fold molar excess of maleimide Oregon Green 488 (Molecular Probes) was incubated with proteins overnight. Unreacted label was quenched by adding 10 mM β-mercaptoethanol and removed by buffer exchange into ddH₂O on G-25 columns and concentrated using a 3000 MWCO membrane (Amicon Ultra; Millipore). The protein was flash frozen and stored at –80 °C. Labeling efficiency was determined to be in excess of 95% by determining the concentration of MdCtC or MdΔ129–148CtC using the Micro BCA Protein assay kit (Thermo Pierce) and Oregon Green by measuring absorption at 496 nm (extinction coefficient = 70,000 M⁻¹ cm⁻¹). The molecular weight of all purified polypeptides was confirmed using mass spectroscopy.

Fluorescence Measurements—For thioflavin T (ThT) binding to fibrils, protein samples were mixed with 10 μM ThT and fluorescence was measured using the Spex Fluorolog-3 (Jobin-Yvon) with an excitation wavelength of 442 nm and emission

wavelength of 482 nm. For time-dependent fibrilization measurements, acrylodan was measured in Spex Fluorolog-3 using an excitation wavelength of 380 nm and an emission wavelength of 460 nm. Alternatively, multiple fibrilization reactions were carried out in a volume of 100 μl in black, clear flat-bottom, nonbinding 96-well plates (Corning). Fluorescence was measured in a FLUOstar Omega (BMG LABTECH GmbH) fluorescence plate reader equipped with 380-nm excitation and 460-nm emission filters. Measurements were taken at 10-min intervals using 100 flashes per read. Alternatively the Enspire 2300 Multilabel Reader (PerkinElmer Life Sciences) was used. Sample excitation at 380 nm and emission were recorded at 480 nm using 100 flashes per read. For fluorescence anisotropy experiments, Hsp104^{Trap} was added to 0.2 μM Oregon Green 488-labeled MdCtC or MdΔ129–148CtC with ATP. The change in anisotropy was then recorded for 1 h using a BMG PheraStar plate reader until equilibrium was achieved. To determine the relative anisotropy change the baseline of labeled probe in the absence of Hsp104^{Trap} was subtracted from the final equilibrium values. Dissociation constants were determined by fitting individual curves of three independent experiments and the mean ± S.D. reported.

Hsp104 Binding to Md—Hsp104^{Trap} at different concentrations was preincubated in 25 mM HEPES, pH 7.6, 50 mM KCl, 10 mM MgCl₂, 2 mM ATP, 10 mM DTT for 30 min in microplates. To each well, Oregon Green-labeled polypeptides in ddH₂O containing 10 mM DTT were added to a final concentration of 0.3 μM. Anisotropy change was monitored for 1 h using a BMG PheraStar fluorescence plate reader. Plates were read every 102 s with excitation at 485 nm and emission at 520 nm. The change in anisotropy between initial values and those at equilibrium were used to generate binding curves.

In Vitro Fibrilization—Spontaneous and chaperone-dependent fiber formation was performed in fibrilization buffer (FB; 150 mM NaCl, 25 mM HEPES, pH 7.5) or inhibitory buffer (FIB; 5 mM KCl, 25 mM HEPES, pH 7.5) or FIB+ (FIB with 2% glycerol, 0.006% Tween 20) by slow (10 rpm) overhead rotation (Roller Drum TC-7, New Brunswick) or without rotation overnight at room temperature. NM was present at a concentration of 3 μM. Chaperone-dependent reactions were performed in FIB+ containing 2 mM ATP, an ATP regenerating system (20 mM phosphocreatine, 6 units of creatine phosphokinase), 0.6 μM (monomers) each of Hsp104, huHsp70, and Ydj1, and 3 μM total NM. For seeded reactions, preformed fibers were sonicated and a 15 nM final concentration was added to 3 μM unpolymerized N-domain. For inhibition by Md or its derivatives all peptides were filtered, and their concentrations were determined before addition to fibrilization reactions.

TEM Microscopy—Samples were briefly dialyzed against water and dispersed onto carbon films and stained with uranyl acetate. Grids were observed on a Hitachi 8700 transmission electron microscope (Hitachi Science Systems Ltd.) with an acceleration of 75 kV and a beam current of 25 amp. Images were recorded with an AMT-digital camera system (Advanced Microscopy Techniques, Corp.).

Other Methods—Peptide array synthesis and Hsp104 binding, soluble peptide synthesis, fRCMLa binding, and ATPase

Hsp104-mediated Curing of $[PSI^+]$ Prion

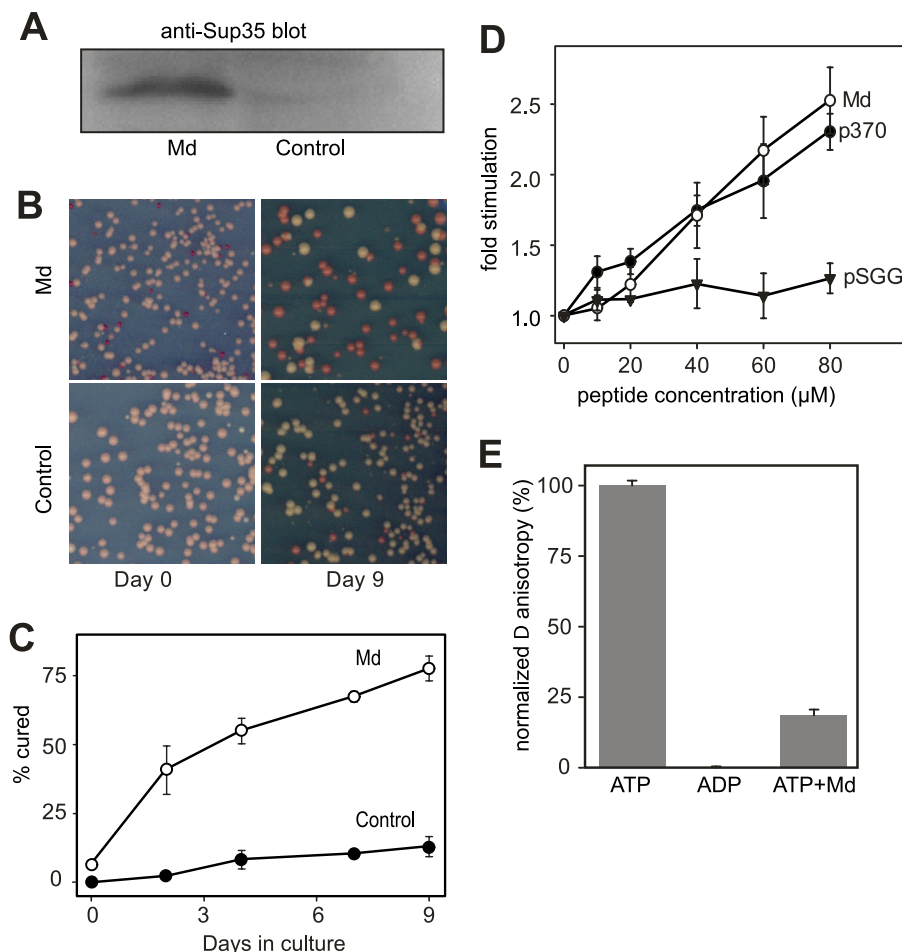


FIGURE 1. Sup35 Md destabilizes $[PSI^+]$ *in vivo* and functionally interacts with Hsp104. *A*, Western blot of copper-induced Md expression in yeast strain OT55. The protein concentrations of extracts were equalized prior to loading. Yeast harboring a plasmid lacking an insert was used as control. *B*, Md expression was induced by growth in medium containing copper and cultures were diluted daily to maintain growth. At intervals, aliquots of cells were washed to remove residual copper and plated on medium lacking copper. Day 0 and day 9 plates are shown. *C*, the number of red-pigmented colonies (cured) on all plates was scored as a percentage of the total number of colonies counted. *D*, the ATPase activity of Hsp104^{E285A} was measured in the presence of Md, the Hsp104-binding peptide p370, and the nonbinding peptide pSGG (35) and expressed as the fold-increase relative to unstimulated activity. *E*, fRCLa binding to Hsp104^{T19P} in the presence of ATP (defined as maximal binding), ADP (no binding), and in the presence of ATP and 7.5 μ M Md.

assays using Hsp104^{E285A} were all performed as previously described (35).

RESULTS

Sup35 Md Destabilizes $[PSI^+]$ *in Vivo* and Interacts with Hsp104 *in Vitro*—We reasoned that if Md contained sites crucial for the propagation of $[PSI^+]$, then overexpression of Md might interfere with $[PSI^+]$ propagation by competing with full-length Sup35 for binding of cellular factors involved in severing pre-existing prion fibrils. To test this hypothesis in a biological context, the coding region of Sup35 amino acids 105–253 was placed under the control of the copper-inducible promoter and expressed in $[PSI^+]$ strain OT55 (16). The expression of the Md was confirmed by Western blotting (Fig. 1A). In $[psi^-]$ cells, high fidelity termination of translation at nonsense codons can prevent the expression of suppressible alleles of genes in the adenine biosynthetic pathway resulting in the accumulation of a red pigmented biosynthetic intermediate (42). In $[PSI^+]$, inefficient termination at nonsense codons permits read-through of nonsense codons resulting in the depletion of the intermediate pool and conferring a pale colony color.

Therefore the loss of $[PSI^+]$ caused by the expression of Md was scored by the appearance of red-pigmented colonies on plates lacking copper indicating the loss of suppression of the *ade1–14* allele present in OT55 (Fig. 1B). The substantial curing effect of Md was established after 2 days in culture and continued until the experiment was terminated (Fig. 1C).

Next we sought evidence that Hsp104 directly interacts with Md. It is known that specific short peptides (13-mers) (35), model unfolded proteins (36, 43), and poly-L-lysine (44, 45) can bind to Hsp104 and stimulate its ATPase activity. For comparison of the effect of Md on Hsp104, we used peptide p370 (KLFSDDDVFEREYA) that has been previously characterized and found to stimulate the ATPase activity in the second AAA+ domain of Hsp104 in a mutant of Hsp104 in which ATP hydrolysis of the first AAA+ domain is inactivated by the substitution of Ala for the catalytic Glu residue in the Walker B motif (Hsp104^{E285A}) (35). We found that Md stimulated the ATPase activity of Hsp104^{E285A} to about the same extent as p370 (Fig. 1D). Previously we demonstrated that p370 inhibits ATP-dependent binding of fluorescently labeled reduced car-

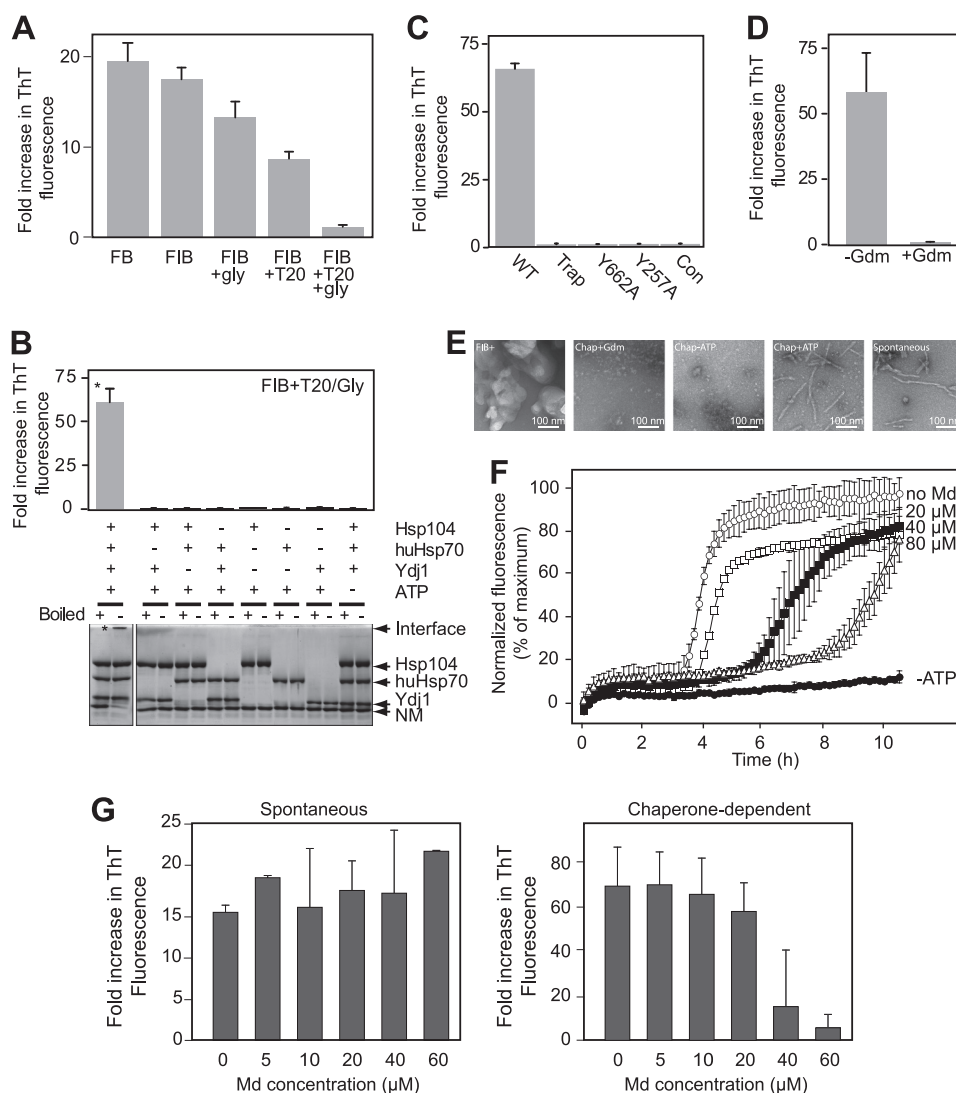


FIGURE 2. Md inhibits chaperone-dependent fibrilization of NM *in vitro*. *A*, 2 μM NM was diluted either into buffers FB or FIB (see “Experimental Procedures”). Tween 20 (T20; 0.03% v/v) and glycerol (gly; 10% v/v) were added to FIB as indicated. After overnight incubation with gentle agitation the increase in ThT binding was determined relative to the initial fluorescence of each reaction. *B*, NM was diluted into reactions into FIB with Tween 20 and glycerol (FIB+) containing molecular chaperones and ATP as indicated. After incubation for 15–17 h in undisturbed reactions, reaction products were analyzed by ThT binding (upper panel; $n = 3$) and SDS-PAGE (lower panel). Proteins in sample buffer were heated either to 99 °C (boiled) or 38 °C to determine SDS resistance. The asterisk in each panel draws attention to the sample with the highest ThT binding and highest SDS resistance indicated by the retention of NM at the interface between the stacking and resolving gels. *C*, reactions in FIB+ containing huHsp70, Ydj1, ATP, and an ATP-regenerating system were conducted in the presence of wild type Hsp104 (WT), Hsp104^{Trap}, Hsp104 with substitutions in pore loops in the second (Hsp104^{Y662A}) or first (Hsp104^{Y257A}) AAA+ domain, or without Hsp104 (CON). *D*, reactions with Hsp104, huHsp70, and Ydj1 were incubated with or without 5 mM guanidinium HCl (Gdm). *E*, negative stain TEM analysis of NM under the following conditions: (left to right) FIB+ with no additions; FIB+ with Hsp104, huHsp70, Ydj1, and 5 mM Gdm; FIB+ with chaperones but no ATP; FIB+ with chaperones and ATP; fibers formed spontaneously in FB. *F*, 3 μM Sup35 NM (25% acrylodan-labeled Sup35Y106C) was incubated in FIB+ with a complete set of chaperones (0.6 μM monomers each), ATP, an ATP regenerating system, and Md. Fluorescence was expressed as a percentage of the maximum fluorescence measured in the control reaction without Md. *G*, left panel, 3 μM NM was incubated in FB for 16 h with gentle agitation in the presence of the indicated concentration of Md. Right panel, 3 μM NM was incubated in FIB+ without agitation along with 0.1 μM Hsp104 hexamers, 0.3 μM Ydj1 dimers, and 0.6 μM huHsp70 monomers, ATP, and an ATP regenerating system, and Md at the indicated concentrations. In both panels fibrilization was determined by ThT fluorescence and expressed as the fold-increase in fluorescence compared with freshly prepared reactions ($n = 3$).

boxmethylated α -lactalbumin (fRCMLa) to Hsp104^{Trap}, a derivative of Hsp104 that can bind but not hydrolyze ATP (35). Md also inhibited fRCMLa binding (Fig. 1E). Together these observations suggest that Md interacts directly with Hsp104 modulating both its ATPase activity and ability to bind an unfolded protein.

Hsp104 has been reported to accelerate the nucleation of NM (24) and full-length Sup35 (46) in reactions that are capable of spontaneous nucleation and to disassemble preformed NM fibrils (24, 25). We experienced difficulty in reproducing these

results and therefore, to determine the role of Md in chaperone-dependent remodeling of Sup35, we developed a novel fibrilization assay that is stringently dependent on the addition of molecular chaperones. We observed that glycerol and Tween 20 together strongly inhibited the spontaneous formation of fibrils by NM in undisturbed reactions (Fig. 2A). Under these conditions, the formation of fibrils was restored by the combined addition of Hsp104, yeast Ydj1, and human Hsp70 (huHsp70) together with ATP (Fig. 2B). The reactions were carried out with huHsp70 rather than yeast Ssa1, which was

Hsp104-mediated Curing of [PSI⁺] Prion

found to be inhibitory to fibrilization (supplemental Fig. S1). No fibrilization occurred in reactions containing either Hsp104^{Trap} or Hsp104 derivatives Hsp104^{Y257A} and Hsp104^{Y662A} lacking conserved tyrosine residues in the proposed axial channel loops in the first and second AAA+ domains, respectively (35) (Fig. 2C). We conclude that the function of Hsp104 in these reactions required both ATP hydrolysis and the ability to process polypeptides via its axial channel. In addition, inhibition of Hsp104 ATPase activity with Gdm (9) inhibited the chaperone-dependent reaction (Fig. 2D).

Transmission electron microscopy showed that the product of the chaperone-dependent fibrilization reactions were fibrils comparable to those spontaneously formed by NM (Fig. 2E). In FIB+ with no chaperones we observed large amorphous aggregates. In reactions that contained chaperones but which did not form fibrils, either in the absence of ATP or in reactions where Hsp104 activity was inhibited by Gdm, NM was deposited as smaller amorphous aggregates. The additives in this system (Tween 20 and glycerol) may promote the formation of off-pathway assemblies that sequester enough NM to indefinitely delay the formation of nuclei that template fibril growth (47). Indeed, a small amount of sonicated NM fibrils restored fibrilization in FIB+ in the absence of chaperones (supplemental Fig. S2).

Using an acrylodan-labeled derivative of NM (29) we were able to follow the time course of fibrilization (supplemental Fig. S3A). The time course of fibril formation measured by this method corresponded to the acquisition of ThT binding (supplemental Fig. S3B) and the formation of SDS-resistant high-molecular weight aggregates of unmodified NM in parallel reactions (supplemental Fig. S3C). The addition of purified Md to chaperone-dependent reactions substantially delayed fibril formation in a concentration-dependent manner (Fig. 2F). In contrast, spontaneous fibrilization was not altered by the addition of Md (Fig. 2G) eliminating the possibility that Md “poisons” the reactions by binding to the growth surfaces at the end of fibrils and blocking further protomer addition. These results are consistent with the idea that Md competes with NM for Hsp104 binding although we cannot exclude the possibility that other chaperones present in the reaction are also affected by Md.

Zeroing in on an Hsp104 Interaction Site in Md—When we probed an array of overlapping peptides corresponding to the NM sequence of Sup35, Hsp104 bound to three regions (Fig. 3A). The first of these (site i; residues 105–119) is located C-terminal to the nonapeptide repeat region of the N-domain and before the highly charged regions of Md. The remaining two sites (site ii, residues 127–147; and site iii, residues 149–165) are within a region of Md that is rich in basic residues. To corroborate the array results, the biochemical properties of Md were characterized in two nonoverlapping segments. Md(105–163) encompassed the basic region of Md including the peptides that bind Hsp104 on arrays. The second segment, Md(164–253), was composed of the more negatively charged region of Md that displayed scant binding of Hsp104. We found that Md(105–163) was a potent inhibitor of chaperone-dependent fibrilization, whereas the Md(164–253) region had no effect (Fig. 3B). Hsp104 ATPase stimulation by Md(105–163)

was similar to full-length Md, whereas stimulation by Md(164–253) was weak (Fig. 3C). fRCMLa binding to Hsp104 was inhibited by Md(105–163) to a similar extent as full-length Md (Fig. 3D). Md(164–253) was 2-fold less potent as an inhibitor compared with either Md or Md(105–163).

Because Md(105–163) contained three putative binding sites for Hsp104 we sought to narrow down the operative region by examining the effect of soluble overlapping 20-mer peptides on the ATPase activity and fRCMLa binding of Hsp104 (Fig. 4). Using the p370 peptide (35) as a standard, conditions were chosen so that we could detect either a comparative increase or decrease in peptide-mediated effects. In these assays, peptides spanning amino acids 126–161 stimulated the ATPase activity of Hsp104 and inhibited fRCMLa binding as well or better than p370. The peptide corresponding to residues 129–148 (FQKQKQAAPKPKKTLKLVLS) was the most potent stimulator of Hsp104 ATPase activity as well as a good inhibitor of fRCMLa binding and was selected for further analysis.

Sup35 Segment 129–148 Is Crucial for Functional Interaction with Hsp104—To test the role of the 129–148 region in conferring an Hsp104 interaction within the context of Md, we examined the properties of an Md derivative lacking these residues (MdΔ129–148). Compared with the intact Md, MdΔ129–148 was a poor stimulator of the ATPase activity of Hsp104 (Fig. 5A). Likewise MdΔ129–148 failed to impair chaperone-dependent NM fibrilization (Fig. 5B). Together these results suggest that the functional interaction between Md and Hsp104 is largely dependent on the 129–148 region.

We next measured the binding of Hsp104^{Trap} to fluorescent Md and MdΔ129–148. There was no detectable Hsp104 binding in the presence of ADP (data not shown). Curve fitting to single site model suggested that the affinity of ATP-dependent Hsp104 binding to the MdΔ129–148 was only subtly decreased (Fig. 5C) perhaps suggesting that the 129–148 segment plays a more important role in regulating the ATPase activity of Hsp104 than in binding.

To complement these findings, we created an NM derivative incorporating the 129–148 deletion (NMΔ129–148). Because the 129–148 deletion does not include any portion of the Sup35 that makes up the amyloid core we anticipated that NMΔ129–148 should be able to spontaneously fibrillize under permissive conditions. Indeed, in overnight, gently agitated reactions, NM and NMΔ129–148 fibrillized to roughly the same extent (Fig. 5D, left panel). However, NMΔ129–148 was refractory to the formation of fibrils in chaperone-dependent reactions (Fig. 5D, right panel). When we compared NM and NMΔ129–148 fibrils seeded with small amounts of preformed NM fibrils, we found that they were morphologically similar and exhibited the same stability when heated in SDS (Fig. 5E). We conclude that the 129–148 region is dispensable for the formation of fibrils that have properties similar to those formed by intact NM, but critically important for chaperone-dependent remodeling of NM that leads to nucleation in our system.

We considered the possibility that to remodel NM, the 129–149 region was required to stimulate the ATPase activity of Hsp104. Addition of the 129–148 peptide to chaperone-dependent fibrilization reactions did not stimulate fibrilization of NMΔ129–148 (data not shown) suggesting that the element

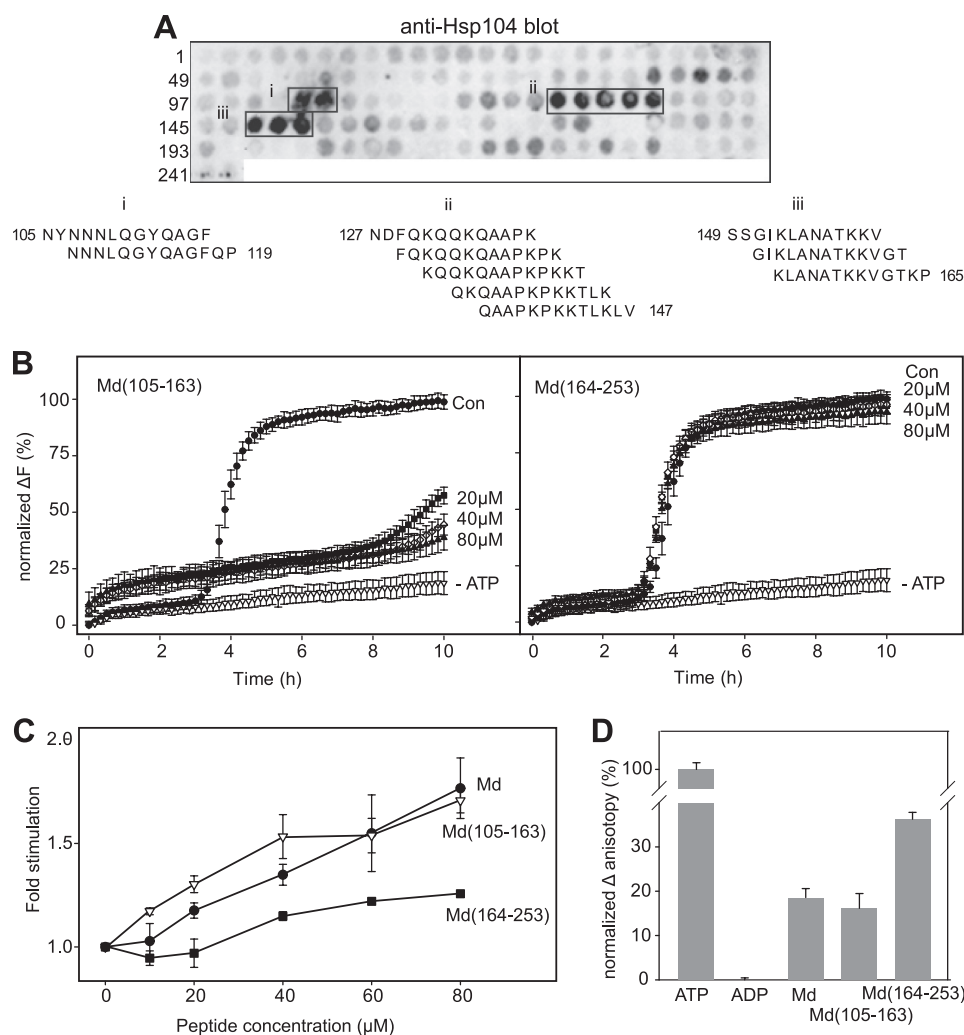


FIGURE 3. The basic region of Md functionally interacts with Hsp104. *A*, overlapping 13-mer peptides spanning the Sup35 N- and M-domains (amino acids 1–253) were spot-synthesized on cellulose membrane and probed with 35 nM Hsp104^{Trp} in the presence of 2 mM ATP. Bound protein was transferred to membrane and detected with anti-Hsp104 antibodies. Three binding regions were identified highlighted on the blot in boxes labeled *i*, *ii*, and *iii* with the amino acid sequences of the Hsp104-binding peptides shown below. *B*, fibrilization of Sup35 NM was carried out as described in the legend to Fig. 2*E* in the presence of polypeptides corresponding to Sup35 residues 105–163 and 164–253. *C*, the ATPase activity of Hsp104 was measured in the presence of various concentrations of Md, and the two subsegments used in panel *B*, and expressed as the fold-increase over activity measured in the absence of proteins. *D*, fluorescence anisotropy was used to measure fRCMLa binding to Hsp104^{Trp} in the presence of ATP, ADP, and in the presence of 7.5 μM Md, Md(105–163), and Md(164–253).

must be present on the remodeled protein and does not function in *trans*. Neither did replacement of the 129–148 region with the amino acid sequence of p370 (which binds Hsp104 and stimulates its ATPase activity) restore chaperone-dependent fibrilization (data not shown) suggesting that the 129–148 sequence has properties that are not replicated by other sequences.

Sup35 Δ 129–148 Is Partially Defective Prion Fragmentation—To test the effect of eliminating the 129–148 region from Sup35 in a biological context, we created a plasmid for the expression of Sup35 incorporating a deletion of this sequence (Sup35 Δ 129–148). Single-copy *LEU2* plasmids for the expression of full-length Sup35 and Sup35 Δ 129–148 were transformed into $[PSI^+]$ yeast strain 780-1D (48) in which viability is maintained by a single copy of *SUP35* present on a *URA3*-marked plasmid. Several independent isolates of each transformed strain were cultured in 5'-fluoroorotic acid to induce the loss of the *URA3*-marked plasmid (Fig. 6*A*). After plasmid shuffling, the expression of Sup35 and Sup35 Δ 129–

148 was analyzed by Western blotting (Fig. 6*B*). Despite being expressed from the native *SUP35* promoter, Sup35 Δ 129–148 accumulation was higher than full-length Sup35. This discrepancy in steady state accumulation levels was corroborated in three independent isolates from both $[PSI^+]$ and $[psi^-]$ backgrounds (data not shown). Although not normally associated with protein turnover, Hsp104 appears to play a role in the turnover of polyglutamine-expanded ataxin 1 expressed in yeast (49). However, in cycloheximide chase experiments, we found that Sup35 and Sup35 Δ 129–148 were both highly stable proteins and that differential turnover could not explain the discrepancy in expression levels (data not shown).

The suppression phenotype (pale colony pigment) of the plasmid-swapped strain expressing full-length Sup35 was identical to the $[PSI^+]$ parental strain (Fig. 6*C*). Yeast expressing only Sup35 Δ 129–148 remained $[PSI^+]$ but exhibited an intermediate level of suppression indicated by the pink colony color (Fig. 6*C*). When we analyzed the SDS-resistant particle size of Sup35 in plasmid-swapped strains, Sup35 maintained the same

Hsp104-mediated Curing of $[PSI^+]$ Prion

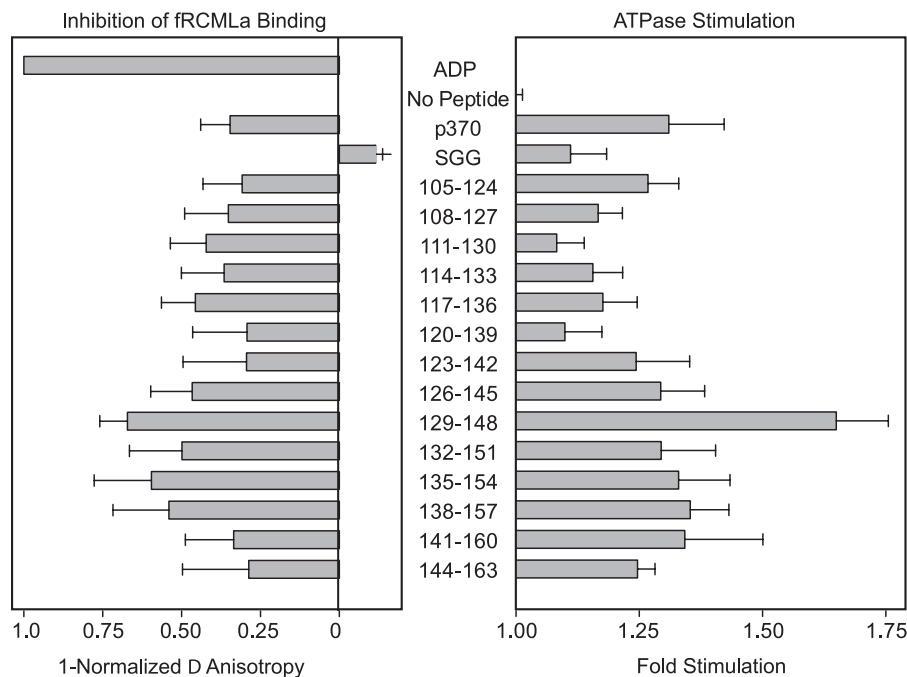


FIGURE 4. **The functional interaction of soluble Md peptides with Hsp104.** Overlapping 20-mer peptides corresponding to the basic region of the Sup35 Md were assayed for Hsp104^{E285A} ATPase stimulation (*right panel*) at a concentration of 26 μM and inhibition of ATP-dependent fRCMLa binding to Hsp104^{Trap} (*left panel*) at a concentration of 7.5 μM . These concentrations were chosen so that the positive control peptide p370 effect was about 50% of its maximum. The nonbinding peptide pSGG was used as a negative control.

particle size as the parental strain, whereas the particle size distribution of Sup35 Δ 129–148 was substantially larger (Fig. 6D).

The larger particle size distribution of Sup35 Δ 129–148 prions may indicate that they are severed less frequently than fibrils composed of intact Sup35, and thus maintain a lower population of propagons. Nonetheless, the $[PSI^+]$ maintained by Sup35 Δ 129–148 is mitotically stable suggesting that new propagons are produced with at least the minimum frequency necessary for continuous transmission to daughter cells. To test whether propagation of the Sup35 Δ 129–148 prion remained dependent on Hsp104, we grew yeast strains in the presence of Gdm to inhibit Hsp104 function (9, 50). $[PSI^+]$ maintained by either full-length Sup35 or Sup35 Δ 129–148 was cured by this treatment confirming that Hsp104 indeed plays a role in propagating both prions (Fig. 6E). However, curing the Sup35 Δ 129–148 prion was faster, indicative that a lower number of propagons are maintained in this strain.

Importantly, overexpression of full-length Sup35 can also mimic the properties we observed in the strain expressing Sup35 Δ 129–148 (51, 52). During the creation of the strain expressing only Sup35 Δ 129–148, we did not notice a pronounced weak suppression phenotype in the intermediate $[PSI^+]$ strain expressing full-length Sup35 and Sup35 Δ 129–148 together (Fig. 6F). We analyzed the Sup35 particle size in this strain and found it to be comparable with the size of particles in the strains expressing either one or two copies of full-length Sup35. When exposed to Gdm the yeast strain expressing two copies of full-length Sup35 and expressing full-length and Δ 129–148 Sup35 together lost $[PSI^+]$ to the same extent (Fig. 6G). From these experiments we conclude that when the prion particles have at least some Sup35 with the 129–148

region intact, they are severed with sufficient frequency to maintain a large population of smaller particles and sequester enough Sup35 to maintain a high level of suppression. Therefore the weaker suppression phenotype and efficient Gdm-mediated curing of the $[PSI^+]$ maintained by Sup35 Δ 129–148 cannot be explained by overexpression alone.

Sup35 Residues 129–148 Are Required for $[PSI^+]$ Curing by Hsp104 Overexpression—We continued to probe the consequences of eliminating Sup35 residues 129–148 by examining the effect of Hsp104 overexpression on $[PSI^+]$ curing. $[PSI^+]$ isolates with either galactose-inducible *HSP104* or the corresponding empty vector were cultured in medium supplemented with either galactose or glucose. Western blot analysis showed Hsp104 expression to be 4–5-fold higher in galactose (Fig. 7A). After overnight growth, about 50% of the colonies were cured when $[PSI^+]$ was maintained by intact Sup35 (Fig. 7, B and C). In contrast, $[PSI^+]$ maintained by Sup35 Δ 129–148 was not cured by Hsp104 overexpression.

When induced by transient overexpression of Sup35, $[PSI^+]$ isolates can exhibit different efficiencies of suppression (53) and mitotic stabilities (54) indicating that, like the mammalian prion, $[PSI^+]$ can exist as different “strains.” “Weak” strains of $[PSI^+]$ have more soluble Sup35 than their strong counterparts and suppression is consequently less efficient (55). The underlying physical distinction among prion strain variants is explained by distinct packing interactions within the core amyloid fibril (28) that are established when fibrils are formed *de novo* and which serve as folding templates during subsequent fiber growth and propagation (41). The weaker suppression phenotype and larger particle size distribution of the prion maintained by Sup35 Δ 129–148 was potentially the result of

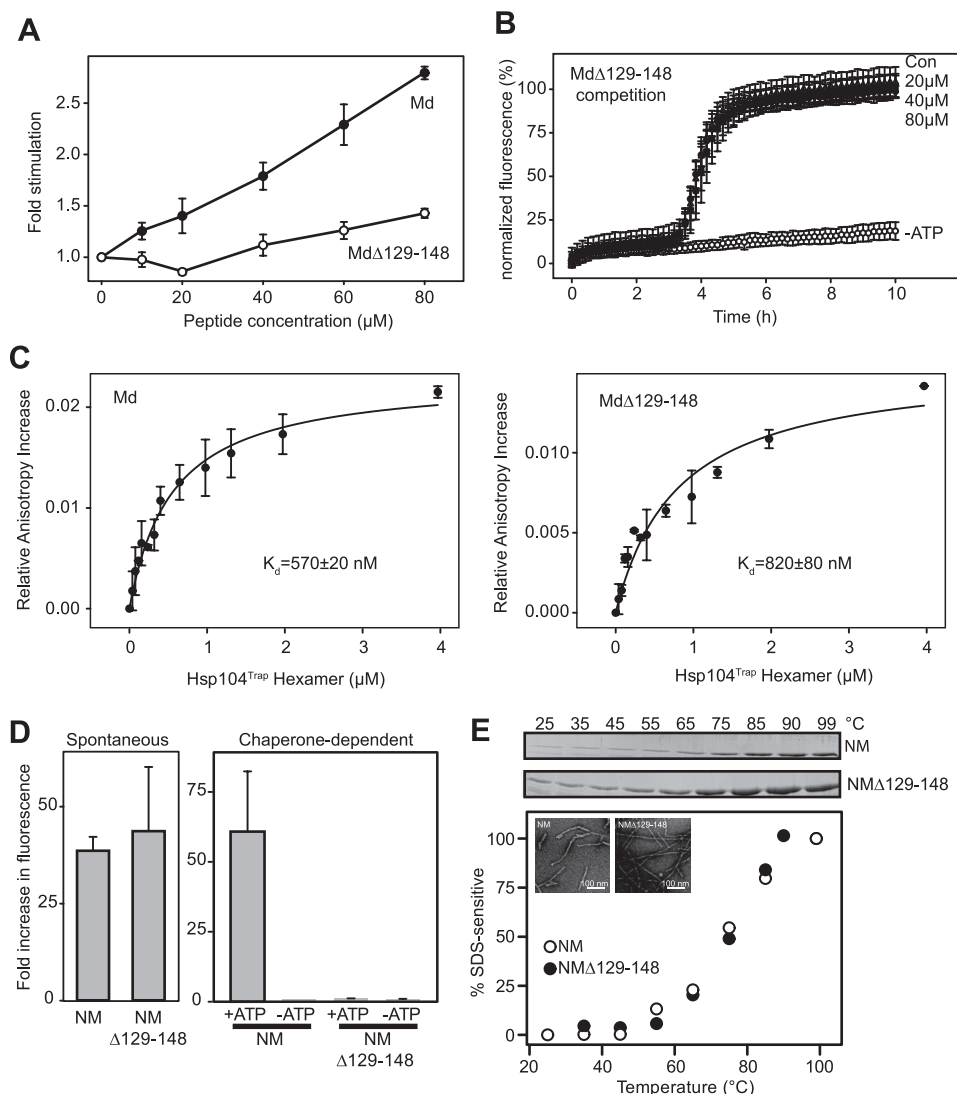


FIGURE 5. Deletion of amino acids 129–148 diminishes functional interactions with Hsp104. *A*, the ATPase activity of Hsp104 was measured in the presence of Md and Md Δ 129–148 and expressed as the fold-increase over activity measured in the absence of peptide. *B*, the fibrilization of 3 μ M NM in the presence of Hsp104, huHsp70, and Ydj1 (0.6 μ M monomers each) was monitored in the presence of increasing concentrations of Md Δ 129–148. The enhancement of acrylodan fluorescence was normalized to the maximum value obtained in reactions without addition of peptide. *C*, the binding of Hsp104^{Trap} to fluorescently labeled Md and Md Δ 129–148 was measured using fluorescence anisotropy in the presence of ATP. *D*, spontaneous and chaperone-dependent fibrilization of intact NM and NM Δ 129–148 were compared. For spontaneous fibrilization, 3 μ M of the each protein was rotated overnight and fibrilization was measured by ThT fluorescence and expressed as the fold-increase in fluorescence in samples compared with the starting material. Chaperone-dependent reactions were as described in *panel B* but ThT fluorescence was used to determine the extent of fibril formation. *E*, comparison of fibrils produced from NM and NM Δ 129–148 seeded with preformed NM fibrils using negative stain TEM (*inset*) and thermal stability of fibrils. *Top panels* show Coomassie-stained gels of proteins entering the gel after heating at the indicated temperature in SDS. *Lower panel* shows quantitation of solubility.

spontaneous switching from a strong to a weak strain of $[PSI^+]$ rather than a diminished Hsp104 interaction.

To test this possibility we reintroduced full-length Sup35 on a *URA3* marker into $[PSI^+]$ strains derived from plasmid swapping in which $[PSI^+]$ had been continuously maintained by Sup35 Δ 129–148. After the elimination of the Sup35 Δ 129–148 expressing plasmid, the particle size distribution of prions now maintained by intact Sup35 was restored to the same size distribution as the original parental strain (Fig. 8*A*). Furthermore, $[PSI^+]$ curing by Hsp104 overexpression was also restored (Fig. 8*B*). Thus, the larger particle size distribution and resistance to Hsp104-mediated curing of $[PSI^+]$ maintained by Sup35 Δ 129–148 is more likely the result of an impaired Hsp104/Sup35 interaction rather than the acquisition of physical properties different from those of the original prion strain.

DISCUSSION

Although the propagation of most known yeast prions depends on Hsp104, curing of Hsp104 overexpression is unique to $[PSI^+]$. Removal of the 129–148 segment of Sup35 confers properties on $[PSI^+]$ that are similar to most other prions, which are dependent on Hsp104 for propagation but resistant to curing by Hsp104 overexpression.

Our initial hypothesis, that Md is involved in propagation and curing of $[PSI^+]$, arises from the assumption that Hsp104 must interact with a part of Sup35 that is accessible when it is assembled into prion particles. The observations that when NM is assembled in fibrils *in vitro*, Md remains largely susceptible to proton exchange (28) and chemical modification (29) make it a good candidate for the interaction. In addition to the biochem-

Hsp104-mediated Curing of $[PSI^+]$ Prion

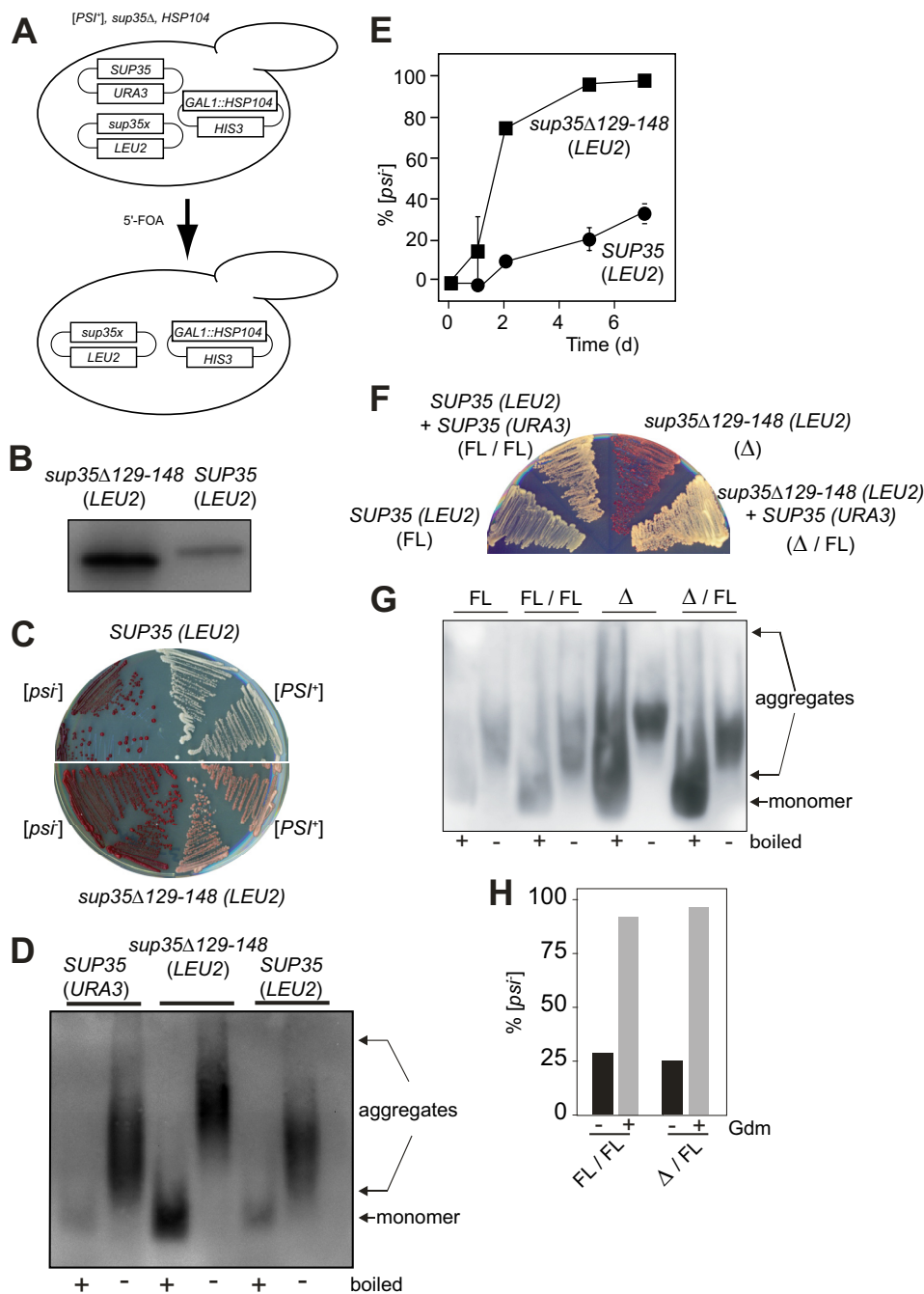


FIGURE 6. *Sup35Δ129-148* displays a propagation defect *in vivo*. *A*, schematic of the plasmid shuffle procedure (see text for a description of the procedures). *B*, after plasmid shuffling, expression of full-length Sup35 and Sup35Δ129-148 was determined by Western blot analysis. *C*, the suppression phenotypes of two isolates each of *[psi⁻]* and *[PSI⁺]* strains were assessed by streaking on 1/4 YPD. *D*, the particle size distributions of SDS-resistant Sup35 in the *[PSI⁺]* parental strain and the plasmid-shuffled strains were analyzed by SDS-PAGE and Western blotting. *E*, Hsp104 dependence of *[PSI⁺]* propagation was examined during continuous culturing of cells in selective media supplemented with 5 mM Gdm. Aliquots were periodically drawn and plated. Red colonies were scored as "cured" and expressed as a percentage of the total number of colonies counted. *F*, suppression phenotypes in "diploid" *[PSI⁺]* intermediates compared with single-copy derivatives. *G*, SDS-PAGE analysis of Sup35 particles in strains shown in panel *F*. *H*, curing of *[PSI⁺]* diploid intermediates after 2 days of growth in 5 mM Gdm.

ical evidence for the accessibility of Md in assembled fibers, experiments in yeast also implicate Md in propagation of *[PSI⁺]* derivatives. *In vivo*, complete elimination of Md results in poor solubility of Sup35ΔM and a highly unstable prion (56). Replacement of Md with a generic charged segment restored solubility to the protein, but the prion maintained by this Sup35 variant was still unstable during mitosis. When Md was

replaced with a linker derived from tropomyosin, mitotic stability, which requires only the occasional severing of prion fibrils, was restored but the resulting prion, *[PSI⁺]^{NTC}*, could not be cured by Hsp104. These observations support the idea that of the two hallmark features of Hsp104 dependence, mitotic stability and curability, curability is more stringently dependent on the presence of an intact Md.

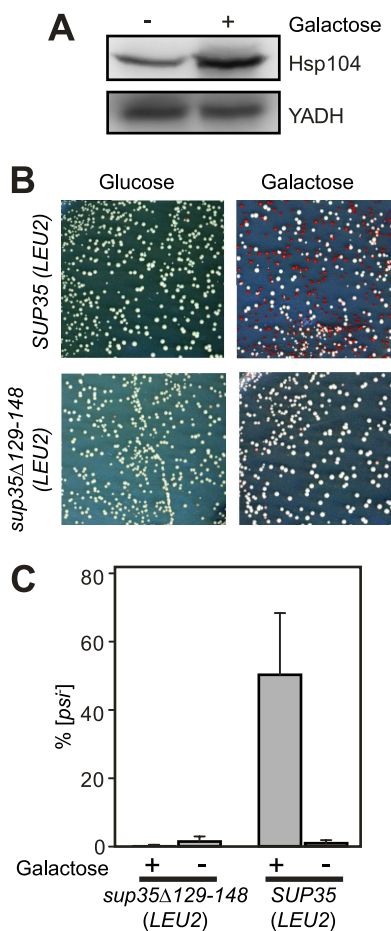


FIGURE 7. $[PSI^+]$ maintained by Sup35 Δ 129–148 is resistant to curing by Hsp104 overexpression. *A*, $[PSI^+]$ cells were cultured overnight in selective medium containing 2% galactose and 0.03% glucose. Galactose-inducible Hsp104 expression was compared by Western blotting to cells grown in glucose. Blots were reprobed with an antibody against yeast alcohol dehydrogenase (YADH) as a loading control. *B*, cells were washed and plated onto glucose-containing selective medium to suppress further Hsp104 overexpression. *C*, red colonies were scored as cured and expressed as a percentage of the total number of colonies counted.

The nonapeptide repeat region has also been implicated in the Hsp104/Sup35 interaction. Progressive reduction in the number of nonapeptide repeats results in $[PSI^+]$ variants that are larger in size and mitotically unstable (57). Others have also reported that $[PSI^+]$ is poorly maintained by Sup35 with reduced numbers of repeats (58, 59). One possible explanation of these results is that the repeat region of Sup35 provides binding sites for Hsp104 or that these deletions affect the accessibility of nearby binding sites. However, scrambling the amino acid sequence of the nonapeptide repeat region resulted in formation of prions with a variety of suppression phenotypes but all of which display normal mitotic stability and Hsp104-mediated curability (60). The conclusion that the nonapeptide repeat region has no sequence specific determinants for Hsp104-mediated curing is consistent with our finding that Hsp104 does not interact peptides derived from this region. Instead the biochemical evidence we have accumulated suggests that Md interacts with Hsp104 both functionally and physically, and that these interactions are influenced by deletion of the 129–148 region.

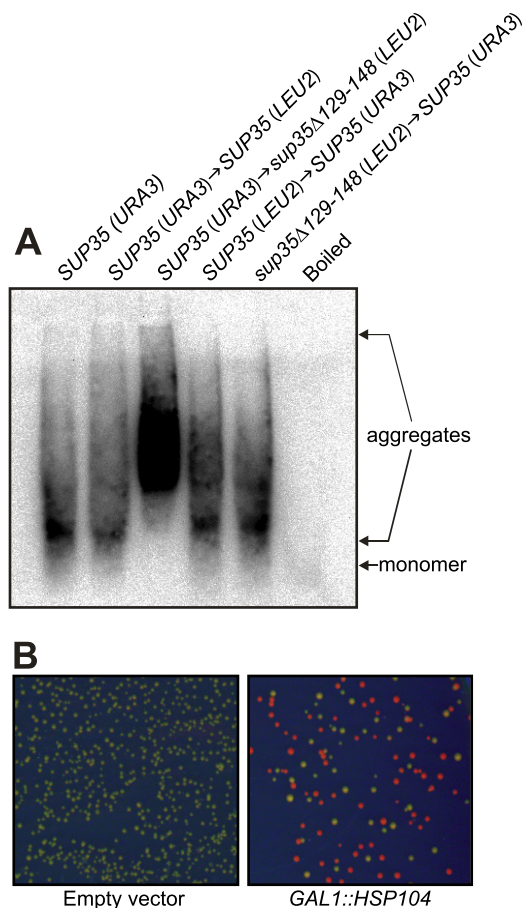


FIGURE 8. $[PSI^+]$ maintained by Sup35 Δ 129–148 is not a different strain. $[PSI^+]$ cells were transformed with a URA3 marked SUP35 plasmid and grown for many generations without selection to induce loss of the LEU2-marked plasmid. *A*, the SDS-resistant Sup35 particle size distributions of the parental strain, the plasmid-swapped strains, and the restored strains were analyzed by SDS-PAGE and Western blotting. *B*, the strain that was restored following the maintenance of $[PSI^+]$ by Sup35 Δ 129–148 was grown overnight as described in the legend to Fig. 7*B*.

In terms of a functional interaction, we found that the ability of Md to inhibit chaperone-dependent fibrilization *in vitro* and the ability of NM to undergo chaperone-dependent fibrilization required the 129–148 segment. In addition we find that Md stimulates the ATPase activity of Hsp104 and inhibits RCMLa binding and that these properties are also impaired by deletion of the 129–148 segment. In terms of a physical interaction, we found that Hsp104 bound to Md-derived peptides on arrays, and that the affinity of Hsp104 binding to Md in solution was diminished when residues 129–148 were absent.

In work that is in progress,³ we find that the affinity of binding peptide p370 to Hsp104 is modulated by substitution of aromatic side chains. Using surface plasmon resonance as an analytical technique, Hsp104 hexamers bind to immobilized p370 with a K_d of ~ 17 nM. Substitution of two Phe residues with Ala abolishes the ability of p370 to stimulate the ATPase activity of Hsp104 and inhibit RCMLa binding concurrent with a ~ 30 -fold reduction in Hsp104 affinity (~ 450 nM). This affinity is in the range measured for Hsp104 binding to Md, which has few aromatic amino acids (~ 570 nM). Even with an affinity of

³ R. Lum, M. I. Michalowska, and J. R. Glover, manuscript in preparation.

Hsp104-mediated Curing of $[PSI^+]$ Prion

Hsp104 binding in the range that largely eliminates the regulatory properties of p370, Md stimulates the ATPase activity of Hsp104 to roughly the same extent as unmodified p370. Elimination of the 129–148 region strongly impacts the ability of Md to stimulate the ATPase activity of Hsp104 even though we measured a relatively modest decrease in binding affinity (~ 870 nM). Thus the simple reduction in binding affinity between Hsp104 and Sup35 does not offer a comprehensive explanation for the marked defect in Hsp104-dependent curing of $[PSI^+]$ maintained by Sup35 Δ 129–148. Propagation, however, which requires very limited remodeling activity, may be less stringently dependent on the 129–148-mediated interaction and is only marginally impacted by its elimination. We propose that the weaker binding conferred by Md in the absence of the 129–148 region is sufficient for propagation, but that curing involves additional activation of the Hsp104 ATP-driven protein-unfolding engine.

The *in vitro* fibrilization assay we used in these studies is more akin to the disaggregation and refolding reactions for various model substrates than to the more biologically relevant fibril severing reaction (24) that we were unable to reproduce. Although it has been proposed that Hsp104 could have a role in promoting nucleation *in vivo* (24, 61) there is little evidence for this idea. As such, the chaperone-dependent nucleation and fibrilization reaction we use in these experiments acts only as an indicator of the capacity of Hsp104 to remodel NM while not replicating a specific biological process. Nonetheless, the outcome of these reactions correlates with the Hsp104-dependent curing of $[PSI^+]$ maintained by Sup35 and Sup35 Δ 129–148. For nucleation to occur in these reactions, the chaperone network is needed to extricate protomers from the amorphous aggregates that are formed by NM in the presence of glycerol and Tween 20. This remodeling process is dependent on the 129–148 segment. It is formally possible on the basis of these data alone that the 129–148 segment could be essential for an interaction with either Ydj1 or huHsp70. But the preponderance of evidence we have accumulated suggests that the requirement for the 129–148 sequence can be attributed to its interaction with Hsp104.

In initial trials we found that the *in vitro* fibrilization reaction was not supported by the yeast cytosolic Hsp70 Ssa1 as has been reported by others using different conditions (46, 62). Hsp104 is known to also form a functional disaggregation network with mammalian Hsp70 family members (34, 63) and substitution of huHsp70 for Ssa1 lead to robust chaperone-dependent fibrilization under our conditions. Recent evidence suggests that Ssa1 together with cytosolic Hsp40s, either Ydj1 or Sis1, is involved in transferring refolding substrates to Hsp104 through an interaction that depends on the Hsp104 coiled-coil domain (64, 65). It is therefore somewhat surprising that Ssa1 inhibited rather than promoted nucleation in these reactions. We found that Ssa1 completely inhibited fibrilization when present at a 10-fold molar excess over other chaperones in the reactions (2-fold molar excess with respect to NM). At lower concentrations it substantially delayed nucleation without much effect on the rate of fibrilization after nucleation had been achieved. Ssa1 could bind to NM in the amorphous aggregated state and inhibit extraction of NM monomers with the efficiency neces-

sary to promote nucleation. Ssa1 could also directly perturb the *de novo* assembly or reorganization of nuclei that initiates the fibrilization phase of the reaction. This is consistent with the observation that Ssa1 is capable of binding to NM in a number of aggregated states in an ATP-dependent interaction that is mediated by either Ydj1 or Sis1 (46). The activity of huHsp70 in these reactions is distinct from that of Ssa1 suggesting that the interaction of Ssa1 with NM may be exceptional relative to the generic interaction of Hsp70s with denatured substrates. Ssa1 interference with fibrilization reactions may be mechanistically similar to the manner in which Ssa1 antagonizes Hsp104-mediated curing of $[PSI^+]$ *in vivo* (40).

Our data point to a specific sequence required for Hsp104-mediated curing. However, there are examples of $[PSI^+]$ variants maintained by full-length Sup35 that are not cured by Hsp104 overexpression. One variant initially created using Sup35 lacking amino acids 22–69 ($[PSI^+]^{\Delta 22/69}$) produces large SDS-resistant particles and is mitotically unstable only on rich medium (66). Hsp104 overexpression increases transmission of the $[PSI^+]^{\Delta 22/69}$ prion rather than eradicating it. This property is preserved when Sup35 Δ 22/69 is replaced by full-length Sup35 indicating that the defect in Hsp104-mediated curing cannot be ascribed to the deleted sequence. Similarly $[PSI^+]^{\uparrow Hsp104}$ is a prion variant selected for transmission only at levels of Hsp104 that would normally cure conventional $[PSI^+]$ (52). The particle size distribution of this prion suggests that it forms very large assemblies that can still be propagated by Hsp104 but that are not cured when Hsp104 is overexpressed. Each of these incurable prions likely represents an extreme variation of the core amyloid packing conformation of Sup35 in the prion state. These prions may either have excessive stability or fold in such a way as to mask the region of Md required for a robust Hsp104 interaction.

We can exclude the idea that overexpression of Sup35 Δ 129–148 alone accounts for the larger particle size of prions. When Sup35 Δ 129–148 was co-expressed with normal amounts of full-length Sup35, we did not observe a shift in the size of SDS-resistant aggregates suggesting that even a relatively small amount of full-length Sup35 incorporated into the prion fibrils was sufficient to maintain the infrequent severing required to keep roughly the same particle size as the parent strain. This supports the interpretation that the larger particle size observed when Sup35 Δ 129–148 is expressed by itself is indeed attributable to a lower rate of particle severing. Although we find that deletion of amino acids 129–148 has a pronounced impact on Hsp104-mediated curing we have not eliminated the possibility that other regions of Md could also influence this phenomenon or that the unexpectedly high expression of Sup35 Δ 129–148 also contributed to the observed resistance to Hsp104-mediated curing.

It is also possible that deletion of the 129–148 region enhances the physical stability of prions. However, fibrils created by seeding unpolymerized NM and NM Δ 129–148 with the same starting structures show the same thermal stability *in vitro*. We also considered the possibility that during maintenance of $[PSI^+]$ by Sup35 Δ 129–148, the prion “mutates” to a strain that is resistant to Hsp104-dependent curing. However, when Sup35 Δ 129–148 is replaced by full-length Sup35 both

the particle size and curability characteristics of the original [PSI⁺] are restored.

Artificial prions induced *de novo* and maintained by Sup35 with an intact *Saccharomyces cerevisiae* Md but with the amyloidogenic N-domain replaced by the corresponding domain from *Pichia methanolica* ([PSI⁺PS]) can be obtained with variation in suppression phenotypes similar to conventional [PSI⁺] strains (67). Although these prions are dependent on Hsp104 for propagation (68), [PSI⁺PS] strains are generally more resistant to Hsp104-mediated curing than conventional [PSI⁺] and are in fact cured by overexpression of other chaperones in a strain-dependent manner. There is no widely accepted model for the mechanism of curing by nondisaggregating chaperones but it is possible that they block seeding surfaces, or enhance the function of Hsp104 circumventing the need for overexpression. Regardless, it is evident that prion proteins interact with many chaperones with distinct binding preferences and that strain-specific curing is highly dependent on how these binding determinants are displayed in the assembled prion and the cellular abundance of the specific chaperones that interact with them.

It is of interest to note that Hsp104 from different yeast species differ in their abilities to maintain [PSI⁺]. For example, *Schizosaccharomyces pombe* Hsp104 fails to propagate Sup35 prions (69), whereas *Candida albicans* is able to do so (70). The existence of natural variability has implications for how the Hsp104/Sup35 interaction may have co-evolved as a system for rapid changes in proteome expression in response to fluctuating environmental conditions. Importantly, the existence of natural variability in the Hsp104/Sup35 interaction might imply that the ability of Hsp104 to disperse amyloid-like aggregates of other proteins could be tailored by engineering these specificity determinants.

Indeed, the ability of Hsp104 to mediate disaggregation of misfolded proteins has generated speculation that it might be used as a therapeutic agent in the treatment of diseases involving aggregation prone proteins such as Parkinson or Huntington diseases (71). However, rather than curing, the propagation of the majority of yeast prions is potentiated by Hsp104, which has obvious implications with respect to the anticipated benefits or pitfalls of any Hsp104-based intervention. The ability of Hsp104 to completely disperse amyloid-like aggregates is likely based on a host of factors including the intrinsic physical stability of the amyloid fold that may be determined, for example, by the extent of bond interactions that engage protomers in the fibrillar assembly, the variability in the tertiary fold that could mask or expose sites that are suitable for an initial Hsp104 interaction, the affinity of Hsp104 binding to its target, the ability of binding to regulate the ATPase activity of Hsp104, and the accessibility of appropriate binding sites for additional chaperones that may either promote or antagonize the function of Hsp104. Understanding the properties of the Hsp104/Sup35 interaction revealed in our work is one step in unraveling the overall molecular mechanism of curing. Further investigation will be required to develop a deeper appreciation of the limitations and potential benefits of Hsp104 in dispersing disease-associated aggregates.

Acknowledgments—We thank the SMART facility Mount Sinai Hospital, Toronto, ON, Canada, and Department of Clinical Medicine for the use of fluorescence plate readers, Yury Chernoff for the yeast strain OT55, Dan Masison for the yeast strain 780-1D, Susan Lindquist for the gift of the anti-Sup35 N-domain antibody, and Lynne Quarmbly for helpful comments on the manuscript.

REFERENCES

- Serio, T. R., Cashikar, A. G., Kowal, A. S., Sawicki, G. J., and Lindquist, S. L. (2001) *Biochem. Soc. Symp.* **68**, 35–43
- Stansfield, I., Jones, K. M., Kushnirov, V. V., Dagkesamanskaya, A. R., Poznyakovski, A. I., Paushkin, S. V., Nierras, C. R., Cox, B. S., Ter-Avanesyan, M. D., and Tuite, M. F. (1995) *EMBO J.* **14**, 4365–4373
- True, H. L., Berlin, I., and Lindquist, S. L. (2004) *Nature* **431**, 184–187
- True, H. L., and Lindquist, S. L. (2000) *Nature* **407**, 477–483
- Jensen, M. A., True, H. L., Chernoff, Y. O., and Lindquist, S. (2001) *Genetics* **159**, 527–535
- McGlinchey, R. P., Kryndushkin, D., and Wickner, R. B. (2011) *Proc. Natl. Acad. Sci. U.S.A.* **108**, 5337–5341
- Byrne, L. J., Cole, D. J., Cox, B. S., Ridout, M. S., Morgan, B. J., and Tuite, M. F. (2009) *PLoS One* **4**, e4670
- Chernoff, Y. O., Lindquist, S. L., Ono, B., Inge-Vechtomov, S. G., and Liebman, S. W. (1995) *Science* **268**, 880–884
- Grimminger, V., Richter, K., Imhof, A., Buchner, J., and Walter, S. (2004) *J. Biol. Chem.* **279**, 7378–7383
- Lee, S., Sielaff, B., Lee, J., and Tsai, F. T. (2010) *Proc. Natl. Acad. Sci. U.S.A.* **107**, 8135–8140
- Wendler, P., Shorter, J., Plisson, C., Cashikar, A. G., Lindquist, S., and Saibil, H. R. (2007) *Cell* **131**, 1366–1377
- Parsell, D. A., Kowal, A. S., Singer, M. A., and Lindquist, S. (1994) *Nature* **372**, 475–478
- Weibezahn, J., Tessarz, P., Schlieker, C., Zahn, R., Maglica, Z., Lee, S., Zentgraf, H., Weber-Ban, E. U., Dougan, D. A., Tsai, F. T., Mogk, A., and Bukau, B. (2004) *Cell* **119**, 653–665
- Lum, R., Tkach, J. M., Vierling, E., and Glover, J. R. (2004) *J. Biol. Chem.* **279**, 29139–29146
- Haslberger, T., Bukau, B., and Mogk, A. (2010) *Biochem. Cell Biol.* **88**, 63–75
- Wegrzyn, R. D., Bapat, K., Newnam, G. P., Zink, A. D., and Chernoff, Y. O. (2001) *Mol. Cell Biol.* **21**, 4656–4669
- Kryndushkin, D. S., Alexandrov, I. M., Ter-Avanesyan, M. D., and Kushnirov, V. V. (2003) *J. Biol. Chem.* **278**, 49636–49643
- Roll-Mecak, A., and Vale, R. D. (2008) *Nature* **451**, 363–367
- Derkatch, I. L., Bradley, M. E., Zhou, P., Chernoff, Y. O., and Liebman, S. W. (1997) *Genetics* **147**, 507–519
- Edskes, H. K., Gray, V. T., and Wickner, R. B. (1999) *Proc. Natl. Acad. Sci. U.S.A.* **96**, 1498–1503
- Patel, B. K., Gavin-Smyth, J., and Liebman, S. W. (2009) *Nat. Cell Biol.* **11**, 344–349
- Du, Z., Park, K. W., Yu, H., Fan, Q., and Li, L. (2008) *Nat. Genet.* **40**, 460–465
- Alberti, S., Halfmann, R., and Lindquist, S. (2010) *Methods Enzymol.* **470**, 709–734
- Shorter, J., and Lindquist, S. (2004) *Science* **304**, 1793–1797
- Shorter, J., and Lindquist, S. (2006) *Mol. Cell* **23**, 425–438
- Newnam, G. P., Birchmore, J. L., and Chernoff, Y. O. (2011) *J. Mol. Biol.* **408**, 432–448
- Derdowski, A., Sindi, S. S., Klaipe, C. L., DiSalvo, S., and Serio, T. R. (2010) *Science* **330**, 680–683
- Toyama, B. H., Kelly, M. J., Gross, J. D., and Weissman, J. S. (2007) *Nature* **449**, 233–237
- Krishnan, R., and Lindquist, S. L. (2005) *Nature* **435**, 765–772
- Glover, J. R., Kowal, A. S., Schirmer, E. C., Patino, M. M., Liu, J. J., and Lindquist, S. (1997) *Cell* **89**, 811–819
- Mumberg, D., Müller, R., and Funk, M. (1994) *Nucleic Acids Res.* **22**, 5767–5768

Hsp104-mediated Curing of [PSI⁺] Prion

32. Hara, H., Nakayashiki, T., Crist, C. G., and Nakamura, Y. (2003) *Genes Cells* **8**, 925–939
33. Abravaya, K., Myers, M. P., Murphy, S. P., and Morimoto, R. I. (1992) *Genes Dev.* **6**, 1153–1164
34. Glover, J. R., and Lindquist, S. (1998) *Cell* **94**, 73–82
35. Lum, R., Niggemann, M., and Glover, J. R. (2008) *J. Biol. Chem.* **283**, 30139–30150
36. Schirmer, E. C., Queitsch, C., Kowal, A. S., Parsell, D. A., and Lindquist, S. (1998) *J. Biol. Chem.* **273**, 15546–15552
37. Tkach, J. M., and Glover, J. R. (2004) *J. Biol. Chem.* **279**, 35692–35701
38. Song, Y., Wu, Y. X., Jung, G., Tutar, Y., Eisenberg, E., Greene, L. E., and Masison, D. C. (2005) *Eukaryot. Cell* **4**, 289–297
39. Gietz, R. D., Schiestl, R. H., Willems, A. R., and Woods, R. A. (1995) *Yeast* **11**, 355–360
40. Newnam, G. P., Wegrzyn, R. D., Lindquist, S. L., and Chernoff, Y. O. (1999) *Mol. Cell Biol.* **19**, 1325–1333
41. Tanaka, M., Chien, P., Naber, N., Cooke, R., and Weissman, J. S. (2004) *Nature* **428**, 323–328
42. Smirnov, M. N., Smirnov, V. N., Budowsky, E. I., Inge-Vechtomov, S. G., and Serebrjakov, N. G. (1967) *Biochem. Biophys. Res. Commun.* **27**, 299–304
43. Schaupp, A., Marcinowski, M., Grimminger, V., Bösl, B., and Walter, S. (2007) *J. Mol. Biol.* **370**, 674–686
44. Cashikar, A. G., Schirmer, E. C., Hattendorf, D. A., Glover, J. R., Ramakrishnan, M. S., Ware, D. M., and Lindquist, S. L. (2002) *Mol. Cell* **9**, 751–760
45. Mackay, R. G., Helsen, C. W., Tkach, J. M., and Glover, J. R. (2008) *Biochemistry* **47**, 1918–1927
46. Krzewska, J., and Melki, R. (2006) *EMBO J.* **25**, 822–833
47. Serio, T. R., Cashikar, A. G., Kowal, A. S., Sawicki, G. J., Moslehi, J. J., Serpell, L., Arnsdorf, M. F., and Lindquist, S. L. (2000) *Science* **289**, 1317–1321
48. Wu, Y. X., Greene, L. E., Masison, D. C., and Eisenberg, E. (2005) *Proc. Natl. Acad. Sci. U.S.A.* **102**, 12789–12794
49. Lee do, H., and Goldberg, A. L. (2010) *Biochem. Biophys. Res. Commun.* **391**, 1056–1061
50. Jung, G., and Masison, D. C. (2001) *Curr. Microbiol.* **43**, 7–10
51. Allen, K. D., Wegrzyn, R. D., Chernova, T. A., Müller, S., Newnam, G. P., Winslett, P. A., Wittich, K. B., Wilkinson, K. D., and Chernoff, Y. O. (2005) *Genetics* **169**, 1227–1242
52. Borchsenius, A. S., Müller, S., Newnam, G. P., Inge-Vechtomov, S. G., and Chernoff, Y. O. (2006) *Curr. Genet.* **49**, 21–29
53. Derkatch, I. L., Chernoff, Y. O., Kushnirov, V. V., Inge-Vechtomov, S. G., and Liebman, S. W. (1996) *Genetics* **144**, 1375–1386
54. Kochneva-Pervukhova, N. V., Chechenova, M. B., Valouev, I. A., Kushnirov, V. V., Smirnov, V. N., and Ter-Avanesyan, M. D. (2001) *Yeast* **18**, 489–497
55. Uptain, S. M., Sawicki, G. J., Caughey, B., and Lindquist, S. (2001) *EMBO J.* **20**, 6236–6245
56. Liu, J. J., Sondheimer, N., and Lindquist, S. L. (2002) *Proc. Natl. Acad. Sci. U.S.A.* **99**, Suppl. 4, 16446–16453
57. Shkundina, I. S., Kushnirov, V. V., Tuite, M. F., and Ter-Avanesyan, M. D. (2006) *Genetics* **172**, 827–835
58. Osheroovich, L. Z., Cox, B. S., Tuite, M. F., and Weissman, J. S. (2004) *PLoS Biol.* **2**, E86
59. Parham, S. N., Resende, C. G., and Tuite, M. F. (2001) *EMBO J.* **20**, 2111–2119
60. Toombs, J. A., Liss, N. M., Cobble, K. R., Ben-Musa, Z., and Ross, E. D. (2011) *PLoS One* **6**, e21953
61. Patino, M. M., Liu, J. J., Glover, J. R., and Lindquist, S. (1996) *Science* **273**, 622–626
62. Shorter, J., and Lindquist, S. (2008) *EMBO J.* **27**, 2712–2724
63. Mosser, D. D., Ho, S., and Glover, J. R. (2004) *Biochemistry* **43**, 8107–8115
64. Sielaff, B., and Tsai, F. T. (2010) *J. Mol. Biol.* **402**, 30–37
65. Miot, M., Reidy, M., Doyle, S. M., Hoskins, J. R., Johnston, D. M., Genest, O., Vitery, M. C., Masison, D. C., and Wickner, S. (2011) *Proc. Natl. Acad. Sci. U.S.A.* **108**, 6915–6920
66. Borchsenius, A. S., Wegrzyn, R. D., Newnam, G. P., Inge-Vechtomov, S. G., and Chernoff, Y. O. (2001) *EMBO J.* **20**, 6683–6691
67. Kushnirov, V. V., Kryndushkin, D. S., Boguta, M., Smirnov, V. N., and Ter-Avanesyan, M. D. (2000) *Curr. Biol.* **10**, 1443–1446
68. Kushnirov, V. V., Kochneva-Pervukhova, N. V., Chechenova, M. B., Frolova, N. S., and Ter-Avanesyan, M. D. (2000) *EMBO J.* **19**, 324–331
69. Sénéchal, P., Arseneault, G., Leroux, A., Lindquist, S., and Rokeach, L. A. (2009) *PLoS One* **4**, e6939
70. Zenthon, J. F., Ness, F., Cox, B., and Tuite, M. F. (2006) *Eukaryot. Cell* **5**, 217–225
71. Vashist, S., Cushman, M., and Shorter, J. (2010) *Biochem. Cell Biol.* **88**, 1–13